

Intercomparison of laboratory radiance calibration standards

Betina Pavri, Tom Chrien, Robert Green, and Orlesa Williams

Jet Propulsion Laboratory, California Institute of Technology, Pasadena, California

Abstract: Several standards for radiometric calibration were measured repeatedly with a spectroradiometer in order to understand how they compared in accuracy and stability. The tested radiance standards included a NIST 1000W bulb and halon panel, two calibrated and stabilized integrating spheres, and a cavity blackbody. Results indicate good agreement between the blackbody and 1000W bulb/spectralon panel. If these two radiance sources are assumed correct, then the integrating spheres did not conform to their manufacturer-reported radiances in several regions of the spectrum. More detailed measurements are underway to investigate the discrepancy.

INTRODUCTION

The radiometric calibration of AVIRIS (Airborne Visible/InfraRed Imaging Spectrometer) is a process which is constantly being refined. For the past several years, an Optronics 1000W NIST-traceable bulb and 12" Labsphere Spectralon panel (Figure 1) have been used to provide a radiometric standard for laboratory and runway calibrations of the instrument (Chrien et al., 1995). As specified by NIST, the lamp is positioned 50cm from the panel.

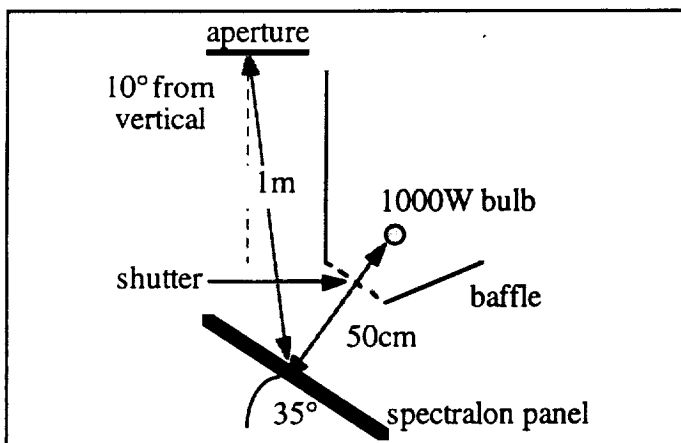


Figure 1: AVIRIS calibration fixture

There are many possible radiometric calibration sources which might provide increased accuracy or stability. Among these are stabilized integrating spheres and calibrated blackbody sources. Two new Optronics integrating sphere sources were purchased and compared to the current standard in the laboratory. An Analytical Spectral Devices full-range (ASD FR) spectroradiometer with a bare fiber

bundle input was used to collect the comparison data. Sources were measured over a period of several hours, and the results were compared.

ANALYSIS

Radiance Calculation

The spectroradiometer has an adjustable dynamic range based on an adjustment to the integration time in the VIS/NIR, and changes to gain and offset beyond 1000 nm. However, since all data sets were collected without changing these settings, the DN levels are directly comparable. They can be used to derive radiance curves for each source, if one radiance source is considered to be the standard. The new integrating spheres were chosen as the standards for the first part of the experiment: measuring the lamp/panel radiance:

$$L_{\text{panel/lamp}} = L_{\text{sphere}} \cdot \frac{dn_{\text{panel/lamp}}(\lambda)}{dn_{\text{sphere}}(\lambda)}$$

Fifty such spectra were averaged to produce the reported results for the lamp and panel.

This radiance could then be compared to the radiance expected from the lamp/panel combination based on the manufacturer's calibration data for lamp irradiance and panel reflectance (Figure 2).

$$L_{\text{panel theoretical}} = \frac{I_{\text{lamp}} \cdot R_{\text{panel}}}{\pi}$$

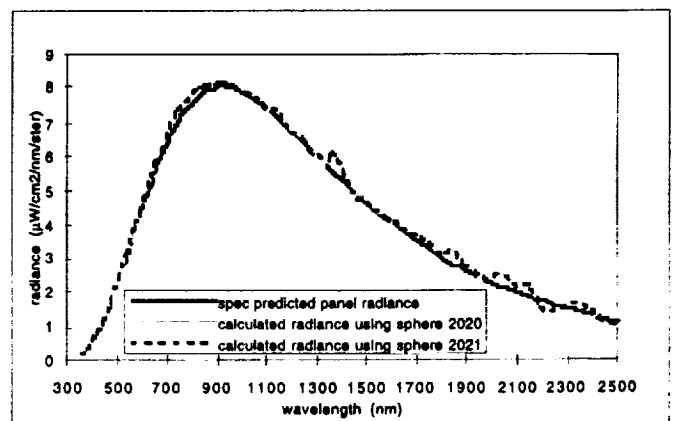


Figure 2: panel radiance from sphere standard

RESULTS

The fit is poor. There are two explanations for this. The first is that the panel and lamp were poorly calibrated by the manufacturers, and the second is that the reported sphere radiances are incorrect. Since both spheres give essentially the same result for panel radiance, this would imply that the spheres share a common calibration error.

A blackbody source was selected to resolve the ambiguity, as it should be free of the kind of water absorptions that occasionally affect spheres and panels used as radiance standards. All three sources were measured using the same spectroradiometer. Blackbody radiances were calculated using both the lamp/panel and a sphere as radiometric standards. The calculated blackbody radiance at several temperatures could then be compared to the theoretical blackbody radiance calculated from the blackbody equation, assuming an emissivity of 1 (Figure 3).

$$L_{\text{ideal}}(\lambda) = \frac{2\pi^5 hc^2}{15} \frac{1}{\lambda^5} \frac{1}{e^{ch/\lambda kT} - 1}$$

where:

- c = speed of light
- k = Boltzmann's constant
- h = Planck's constant
- λ = wavelength of interest
- ϵ = emissivity

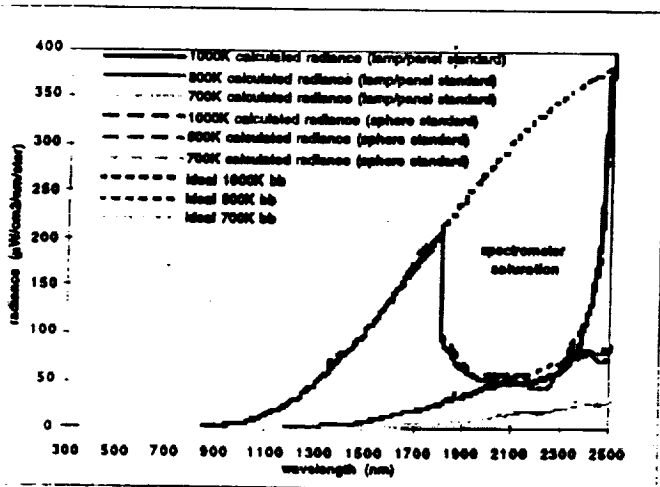


Figure 3: blackbody radiance from lamp/panel and spheres.

The blackbody source saturated the long-wavelength end of the spectroradiometer at high temperature, but good data were obtained from 1000-1800nm for the 700, 800, and 1000 K cases, and over the entire spectrum for the 700 K case.

Note that 1300 nm and 1700 nm discrepancies appear only in sphere-derived spectra in Figure 3.

This is also true for the oscillations between 1800 and 2400 nm in the 700K data. However, the signal levels are low, and the 700K is the only temperature for which data is available for this portion of the spectrum (the higher radiance levels saturated the spectroradiometer).

The fit between the measured and theoretical data for the lamp/panel calibration case is superior to that derived assuming that the spheres were accurately calibrated. Therefore, the discrepancies between the sphere and lamp/panel calibrations are most likely the result of errors in the calibration of the spheres.

The agreement between the theoretical and measured blackbody radiances (using the lamp/panel standard) is examined in detail for the 1000K data in Figure 4:

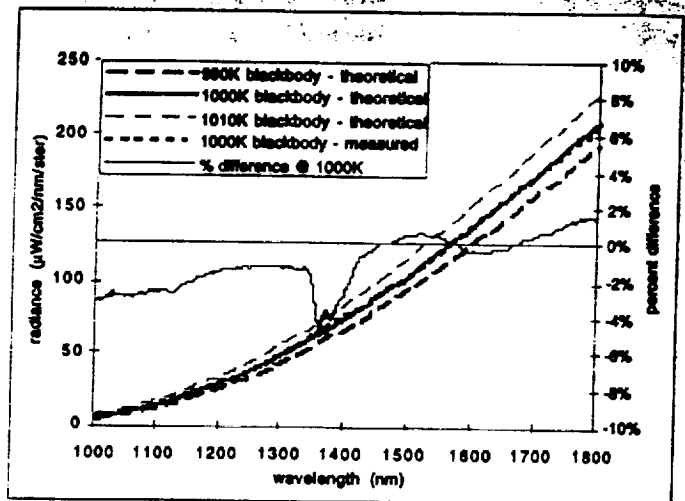


Figure 4: sensitivity of theoretical blackbody radiance to temperature.

Overall, agreement is good. However, there are some issues. A small error in blackbody temperature or emissivity most likely accounts for the small positive slope seen in the percent difference curve. Further, note what is probably atmospheric water vapor absorption artifact from the lamp/panel measurements at ~1350 nm. It introduces error into the radiance derivation, causing the calculated radiance of the blackbody to be underestimated here. This does not explain discrepancies in the integrating sphere data, however, as this spectral feature is offset from the discrepancy observed at 1300 nm in the sphere data, and there is no corresponding feature at 1700 nm.

Radiance of Integrating Spheres

Next, the radiance of the spheres was determined, assuming that the lamp/panel is accurately calibrated. These spectra were compared to the reported sphere radiances, in Figure 5.

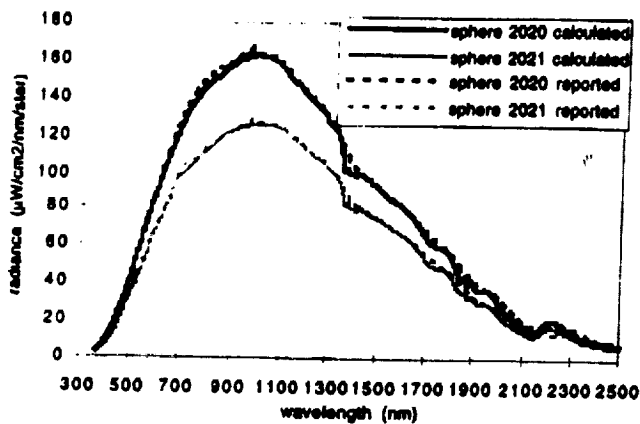


Figure 5: radiance of integration spheres based on NIST 1000W bulb and spectralon panel standard

Note that the manufacturer-reported radiance curves are smoother than the measured results, and that the discrepancies for both spheres track one another (note discrepancies at 1300 nm and 1700 nm). Since the two spheres were calibrated by the manufacturer at the same time, this may be an indication of a problem with the manufacturer's calibration routine, at least for that day. High-frequency "noise" at 1000 nm is most likely due to low response of silicon detector (near its cutoff wavelength) in the spectroradiometer.

The disagreement between measured and reported sphere radiances can be examined by displaying the results as a percent difference (Figure 6).

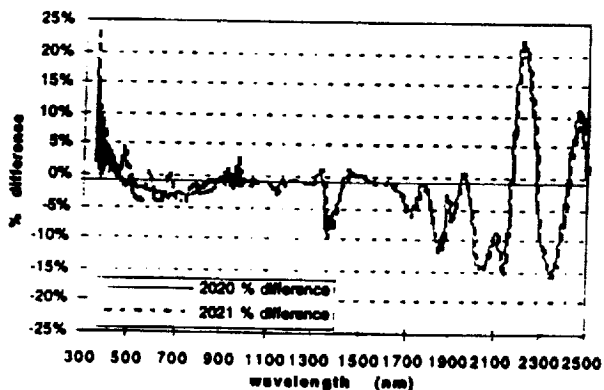


Figure 6: percentage difference between calculated and reported radiance for integrating spheres

Figure 6 indicates discrepancies of up to 20% from the reported radiance values at the long wavelength end of the spectrum. The oscillation from -15% to +20% from 2100 nm to 2300 nm is especially troubling.

Next, the discrepancies in the sphere calibration were checked to establish whether they matched to water vapor or liquid water (Figure 7).

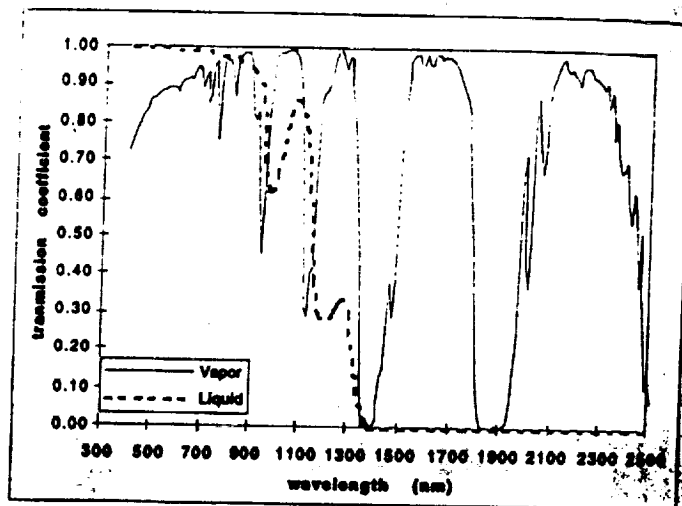


Figure 7: transmission of water (vapor and liquid)

This was done to establish whether the problem is adsorbed water in the sphere surface, or atmospheric water vapor in the light path. Spheres may have significant water vapor signatures due to the large atmospheric path length (due to multiple bounces in the sphere). A quick comparison of both curves to the wavelengths at which the discrepancies occur indicates that water vapor is the main factor. Figure 8 compares the absorptions in the sphere radiance to Modtran-derived water vapor absorptions.

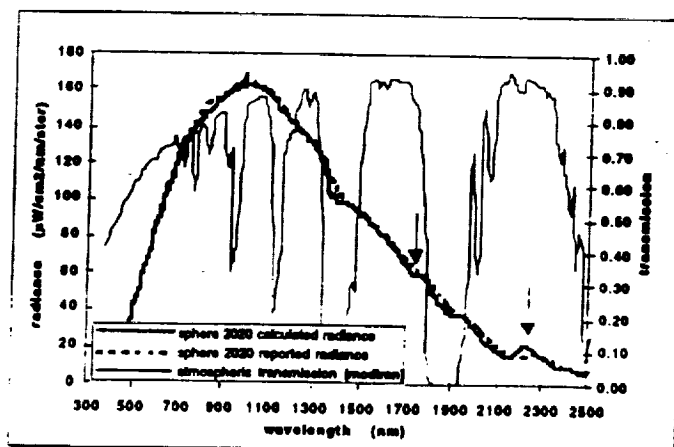


Figure 8: sphere radiance compared to atmospheric transmission, showing influence of water vapor. Arrows indicate discrepancies not explained by water vapor absorption.

So, water vapor apparently accounts for most of the discrepancy, with the exception of two regions of the spectrum. Since radiometric tests are done under ambient conditions, water vapor absorption

will be a critical (and variable) factor in radiometric calibration if spheres are used as the standard.

DISCUSSION

Spectral Calibration:

It is possible that some discrepancies might result if the spectroradiometer were experiencing a spectral shift during measurements. In order to establish whether the instrument was spectrally calibrated, a mercury vapor lamp was observed as part of the test. A series of 100 lamp observations was made in order to accurately determine the spectral offset of the instrument at each emission line. The measured lines were compared to some of the strongest reported emission lines for the lamp (Figures 9 and 10). The results in Figure 9 indicate that the instrument is spectrally calibrated to within 2 nm in the visible/NIR region of the spectrum.

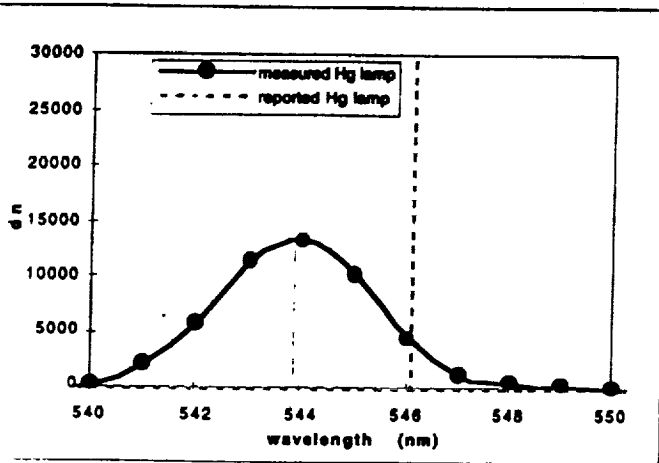


Figure 9: spectral calibration test, visible region.

An IR spectral calibration is shown in Figure 10. Spectral calibration of the spectroradiometer appears to be better here than in the visible.

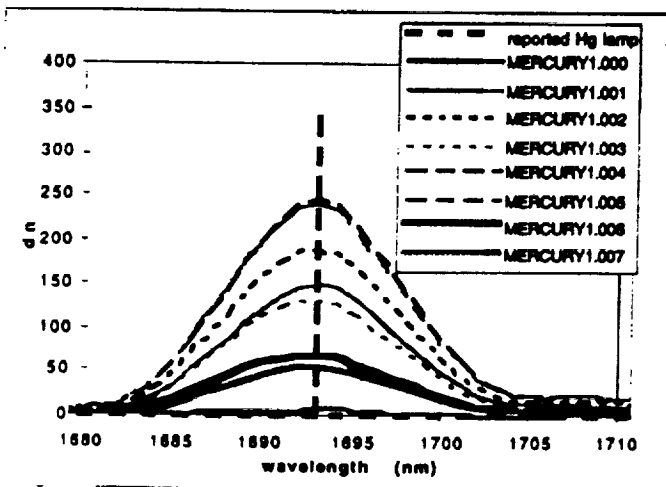


Figure 10: Spectral calibration test, IR region

Further, spectral position is repeatable from measurement to measurement, though absolute DN are not, due to changes in positioning between the lamp and fiber during the period of measurement (both were handheld), and the fact that the lamp did not fill the fiber's FOV.

Verification of Blackbody Temperature:

The assumption of good calibration for the lamp and panel can be checked by independently verifying the blackbody temperature setpoints, assuming the emissivity of the blackbody was very close to 1.0. Microsoft Excel's Solver function was used to minimize the discrepancy between two ratio functions: the ratio of the DN values for the 800K and 1000K ASD measurements of blackbody DN, and the ratio of the theoretical radiance values for two temperature values (T_{high} and T_{low}). T_{high} and T_{low} were allowed to vary. The value to be minimized was the sum-squared of the difference between the two ratios at each wavelength.

Using all points, with 1000K and 800K specified as start points for T_{high} and T_{low} , the results were:

	original temperature	final temperature
T_{high}	1000 K	998.35759 K
T_{low}	800 K	798.118056 K
sum-squared of differences		116.945067

If the apparent water vapor absorption feature between 1300 and 1500 nm (Figure 4) is deleted from the analysis, the program generated this result:

	original temperature	final temperature
T_{high}	1000K	995.813536
T_{low}	800K	796.597793
sum-squared of differences		107.290529

This results in somewhat better agreement (as measured by the sum-squared of differences), and slightly lower temperatures than before.

The accuracy of this method was found to be highly dependent on the starting values chosen for T_{high} and T_{low} . Starting close to the correct values is critical for achieving a sensible result; there probably exist many local minima to this function. The sum-squared of the differences between the two ratios for the final values can be used as a guideline for checking the progress of this process, but this criterion alone is not sufficient to check the results. The residuals between the measured and theoretical radiances would need to be used as well -- so the process is iterative.

CONCLUSIONS

Several radiance standards were compared against one another using a portable spectroradiometer. The results of the testing indicate that the current AVIRIS standard, a 1000W NIST-traceable bulb used in combination with a Spectralon panel, is the most versatile and accurately calibrated of the systems tested. The well-calibrated blackbody may provide a check on the radiance of the bulb/panel, but cannot cover the entire spectral range observed by AVIRIS (400-2500 nm). Water vapor absorptions explain most of the discrepancies between the calculated and manufacturer-reported integrating sphere radiance. However, this does not change the central result for our calibration purposes: these integrating spheres are not a good primary standard for absolute radiometric calibration of hyperspectral systems. The integrating spheres tested may prove more useful if the discrepancies observed are due to a manufacturer calibration error, and if they are stable after calibration is completed. Further tests are underway to determine the stability of all the systems discussed in this paper.

Acknowledgments: This research was carried out at the Jet Propulsion Laboratory/California Institute of Technology, Pasadena, California, under contract with the National Aeronautics and Space Administration. We are grateful to Bruce Kindel for helpful comments on this paper.

REFERENCES

- Chrien, T.G, Green, R.O., Chovit, C., and Hajek, P. (1995), New calibration techniques for the Airborne Visible/Infrared Imaging Spectrometer (AVIRIS). In *Summaries of the Fifth Annual JPL Airborne Earth Science Workshop*, JPL Publ. 95-1, Vol. 1, Jet Propulsion Laboratory, Pasadena, CA, pp. 33-34.